AD-A112 085 FOREIGN TECHNOLOGY DIV WRIGHT-PATTERSON AFB OH F/G 20/4
RELAXATION TECHNIQUES FOR THREE-DIMENSIONAL STEADY TRANSONIC FL--ETC(U)
FEB 82 L YIMIN
UNCLASSIFIED FTD-ID(RS)T-1273-81 NL

END
DATE
FILMED
4 82
DTIC

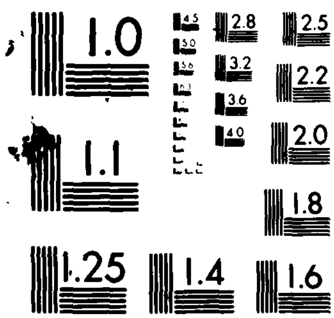

MICROCOPY RESOLUTION TEST CHART
NATIONAL BUREAU OF STANDARDS 1963 A

FTD-ID(RS)T-1273-81

FOREIGN TECHNOLOGY DIVISION

AIR FORCE SYSTEMS COMMAND

RELAXATION TECHNIQUES FOR THREE-DIMENSIONAL STEADY TRANSONIC FLOW ABOUT WINGS

by

Li Yimin

FOREIGN TECHNOLOGY DIVISION

Approved for public release;
distribution unlimited.

EDITED TRANSLATION

FTD-ID(RS)T-1273-81 25 February 1982

MICROFICHE NR: FTD-82-C-000238

RELAXATION TECHNIQUES FOR THREE-DIMENSIONAL STEADY TRANSONIC FLOW ABOUT WINGS

By: Li Yimin

English pages: 8

Source: Acta Mechanica Sinica, Nr. 3, 1981, pp. 296-299

Country of origin: China
Translated by: Randy Dorsey
Requester: FTD/TQTA
Approved for public release; distribution unlimited.

RELAXATION TECHNIQUES FOR THREE-DIMENSIONAL STEADY TRANSONIC FLOW ABOUT WINGS

by Li Yimin

ABSTRACT

Based on difference equations obtained from small perturbation theory and through a hyperbolic tangent transformation which maps the physical space into a cube, the three dimensional steady transonic flow about a wing is computed. Relaxation method reduces the demand on computer memory, and experience is gained through test runs. Calculated results are in good agreement with wind tunnel tests.

In transonic flow simultaneously existing subsonic and supersonic flows along with accompanying shock waves are regarded as characteristic. From the viewpoint of mathematics, the properties of transonic flow must be described by solving "mixed" differential equations which are elliptical in the subsonic region and hyperboloid in the supersonic region. Equation of this type are non-linear and their solution normally involves scontinuous surface -- a shock wave. The best method of dealing wi transonic flows of certain imbedding shock waves is the finite difference relaxation iteration method. Although the first to use the relaxation method to explain transonic flows was Emmons[1], but since he used the Rankine-Hugoniot relationship to set up shock waves, therefore widespread application has not obtained. The finite difference relaxation method which automatically calculates the shock waves which was put forward by Murman and Cole[2] has opened new avenues of research for calculating transonic flow through the flow field.

This paper is based on the characteristic of small perturbations far from the flow about a body (including trailing vortex) to rapidly attenuate, causing the grid to tightly flow about the circumference of the object without affecting the accuracy of the differential operator, and to fully utilize accurate boundary conditions of the distant flow field, particularly using the hyperbolic tangent function coordinate transformation method, an infinitely large physical space is transformed into a perfect cube with side lengths of [-1, +1] within which the finite difference calculations are carried out.

1. TRANSONIC SMALL PERTURBATION DIFFERENTIAL EQUATIONS AND BOUNDARY CONDITIONS

The transonic small perturbation differential equation disregarding high-order small quantities is:

$$\left[1 - M_\infty^2 - (\gamma + 1)\frac{M_\infty^2}{u_\infty}\varphi_{1x_1}\right]\varphi_{1x_1x_1} + \varphi_{1y_1y_1} + \varphi_{1z_1z_1} = 0 \qquad (1)$$

for convenience of calculation, it is expressed as a coordinate transformation, let

$$x = x_1/c, y = y_1/b, z = \delta^{\frac{1}{3}}M_\infty^{2/3}(\gamma + 1)^{\frac{1}{3}}z_1/c$$
$$\varphi = [M_\infty^{2/3}(\gamma + 1)^{\frac{1}{3}}/u_\infty c\delta^{2/3}]\varphi_1$$

after these are substituted into the above equation and arranged, we obtain

$$[K_1 - \varphi_x]\varphi_{xx} + K_2\varphi_{yy} + \varphi_{zz} = 0 \qquad (2)$$

where $K_1 = \frac{1 - M_\infty^2}{[\delta M_\infty^2(\gamma + 1)]^{2/3}}$, $K_2 = \frac{c^2}{b^2[\delta M_\infty^2(\gamma+1)]^{2/3}}$

are similar parameters, c is the wing root half-chord, b is the half-span, δ is the maximum relative thickness of the airfoil.

At the object surface with $Z_{\pm s} = f(x,y)$, flow condition

$\left(\frac{\partial\varphi}{\partial Z}\right)_{\pm s} = \frac{\partial f(x,y)}{\partial x} - \alpha/\delta$ is satisfied, and α is the angle of attack. The Kutta condition is satisfied at the wing trailing edge. Passing through the trailing vortex, φ_x and φ_z are both continuous but φ is discontinuous, its jump value $\Gamma(y) = \oint d\varphi(x, y, \pm 0)$ is independent of x, and φ_{zz} is discontinuous. At the boundary of the distant flow field with other than $x \to \infty$, φ and its first and second order partial derivatives of x, y, and z are all equal to zero. At the trailing vortex with $x \to \infty$, the φ value must be determined on the basis of $\Gamma(y)$ at the trailing vortex. Using the following equation, a constant pressure coefficient can be obtained from :

$$c_p = -\frac{2\delta^{2/3}}{M_\infty^{2/3}(\gamma + 1)^{1/3}}\varphi_x, \quad (3)$$

and after integration, the various aerodynamic quantities can be obtained.

2. DIFFERENCE SCHEME, COORDINATE TRANSFORMATION AND RELAXATION ITERATION

Equation (2) is suitable for finite difference iteration solutions. When $\varphi_x < K_1$, the equation becomes elliptical (subsonic flow) and the central difference scheme is used; when $\varphi_x > K_1$, the equation become hyperbolic (supersonic flow) and the x differential uses a one-sided difference operator. Since the sonic line is a continuous transition line, no special provisions must be made. High order error terms brought on by replacement of differentials by difference operators, give rise to dissipative effects; consequently, this can cause the weak shock waves whose intensities and positions were previously unknown, to form "naturally" in the process of solution. This method is called the shock wave capture method. In order to allow large changes in grid density in the flow about the vicinity of the object without reducing the accuracy of the solution, we employed in this paper the hyperbola tangent function coordinate transformation method: $\xi = \text{th}\,\alpha x,\ \eta = \text{th}\,\beta y,\ \zeta = \text{th}\,\gamma z$, and the infinitely large space is changed into a perfect cube with side lengths of ± 1. The changes are a one-to-one correspondence. When $\alpha, \beta, \gamma \geqslant 1$ (this does not lose its generality), the original points are situated in the flow about the object in the center of the calculated space and occupy 76% of the space of the perfect cube. After coordinate conversion, equation (2) can be written as:

$$\alpha^2(1 - \xi^2)[K_1 - \alpha(1 - \xi^2)\varphi_\xi][(1 - \xi^2)\varphi_{\xi\xi} - 2\xi\varphi_\xi] + K_1\beta^2(1 - \eta^2)[(1 - \eta^2)\varphi_{\eta\eta} - 2\eta\varphi_\eta] + \gamma^2(1 - \zeta^2)[(1 - \zeta^2)\varphi_{\zeta\zeta} - 2\zeta\varphi_\zeta] = 0 \quad (4)$$

Calculating change coefficient linear differential equation (4) is not nearly so difficult as equation (2). Here we omitted solution of approximate potential volume integrals for finite far-side values, which has greatly saved computer time. This partial computation corresponds to the time required to solve total flow field iteration [3].

An isometric grid is marked off in the perfect cube, corresponding to a non-isometric grid of great density in the vicinity of the flow about the object in the physical space. For each grid point a difference equation is established and the linear relaxation iteration method is used[4]. The relaxation lines are parallel to the ζ axis. The potentials for points in the proximity of the relaxation line are regarded as known values for solving the sets of difference equations. After the potential $\varphi^{(n)}$ is determined for the n^{th} iteration, $\varphi^{(n+1)}$ calculated on the basis of iteration formula $\varphi^{(n+1)} = \omega\bar{\varphi}^{(n+1)} + (1-\omega)\varphi^{(n)}$ is taken as the initial value, replacing $\varphi^{(n)}$ on the relaxation line. In the equation, ω is the relaxation factor, in the subsonic region $1 \leq \omega < 2$ (super relaxation), and in the supersonic region $0 < \omega \leq 1$ (low relaxation). As soon as preliminary estimates of the φ values are made, the iteration scan can be carried out. Beginning at the section with greatest η value, we scan from the upstream boundary toward the downstream boundary. After scanning to the line where $\eta = 0$ we again scan one section at a time along the η value or small direction until the entire flow field has been scanned, then we consider that one iteration is complete. After each iteration, we use the values for this iteration to determine the circulation distribution. The φ obtained at the Trefftz plane is taken as the boundary value of the lower iteration. After iteration is carried out a certain number of times, if every point in the flow field satisfies $|\varphi^{(n)} - \varphi^{(n-1)}| < \varepsilon$ (ε is control precision, generally taken as 10^{-5}), then we consider that the solution is convergent. The optimum value range of ω confirmed by many numerical tests: super relaxation factor $1.3 \leq \omega \leq 1.8$, for example, $\omega = 1.7$ saves 1/3 the computer time of $\omega = 1$; the low relaxation factor $0.5 \leq \omega \leq 0.8$. In the process of the calculations, if all the points on the entire relaxation line are subsonic points, then the set of difference equations will be linear; if supersonic points occur on the relaxation line, then they will be nonlinear. Now, relatively close values should be used for solving initial value iteration. For example, results obtained when we begin with a certain subcritical M_∞ are used to calculate initial values for relatively high M_∞ (the Mach number climbing method). Numerical tests indicate that so long as the ω value initially selected is low, we can still start with $M_\infty = 0$ to calculate φ under high subcritical M_∞. Under supercritical conditions, if the Mach number climb interval is too great, such as $\Delta M_\infty \gtrsim 0.3$, there is the possibility of resulting in iteration divergence. In this case the climb interval should immediately be decresed and iteration continued. Computer time is directly proportional to the $(1 + r)^{th}$ power of the grid point ($0.4 \lesssim r \lesssim 0.5$ and directly proportional to the logarithm of control precision ε.

3. CALCULATED RESULTS

In this paper we have calculated pressure distributions for rectangular wings with a 6% double circular-arc airfoil and an aspect ratio of 4, wings with a constant chord and 30° sweep-back, as well as rectangular wings with a 5% double circular-arc airfoil and an aspect ratio of 3. From the illustrations it can be seen that our calculated results coincide well with the test results in [5] and [8] and coincide with the results calculated in [6] and [7]. The results of subcritical to supercritical and zero angle of attack to having an angle of attack coincide very well with test results. This is because of difference scheme of low precision was used in the supersonic region and the flow in the vicinity of the leading edge and in the shock wave region undergoes rather drastic changes. The method employed in this paper decreases computer time by approximately one-half that of [6]. Taking the results in Fig. 1 as an example, the 19X10X19 grid points used in this paper involved a computer time of 18 minutes on a 655 machine, but the 50X50X20 grid points used in [6] involved a computer time of 30 minutes on an IBM 360/67. Surface relaxation was also tested in this paper. Surface relaxation was faster than linear relaxation.

The difficulty encountered in calculating three-dimensional transonic flow is how to deal with boundary conditions for complicated profiles. Of particular difficulty are linearizing boundary conditions for working out solutions in the vicinity of a blunt leading edge and improving calculations for swept-back shock waves.

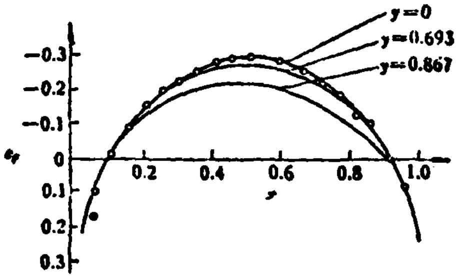

Fig. 1. Constant pressure distribution for a rectangular wing with a 6% double circular-arc airfoil and an aspect ratio of 4.
o test values [5], ——— calculated values for this paper, y is the half-span section, M_∞ = 0.806, α = 0°, subcritical

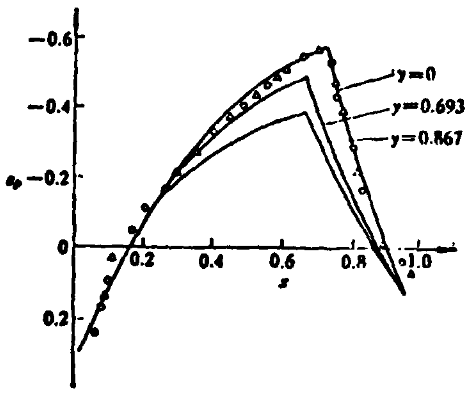

Fig. 2. Constant pressure distribution for a rectangular wing with a 6% double circular-arc profile and an aspect ratio of 4.

o test values[6], y = 0, ▲ test values (two-dimensional)[5],
——— calculated value for this paper, M_∞ = 0.908, α = 0°, supercritical.

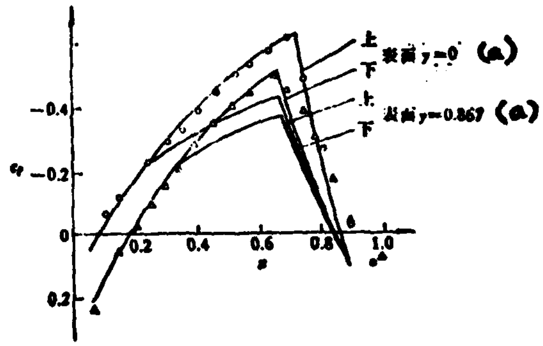

Fig. 3. Constant pressure distribution for a rectangular wing a 6% double circular-arc airfoil and an aspect ratio of 4.

o upper } surface test values[5]
▲ lower }
——— calculated values for this paper, M_∞ = 0.908, α = 1°, supercritical.

KEY: (a) upper / lower surface

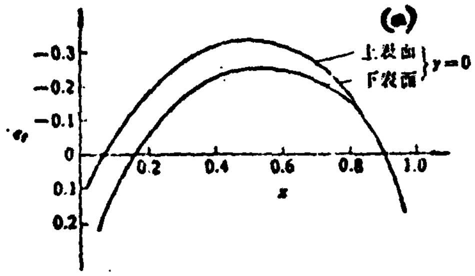

Fig. 4. Wing root cross-sectional pressure distribution for a 30° swept-back wing with a 6% double circular-arc profile and an aspect ratio of 4.

$M_\infty = 0.808$, $\alpha = 1^\circ$, $y = 0$, subcritical

KEY: (a) upper surface, lower surface } y = 0

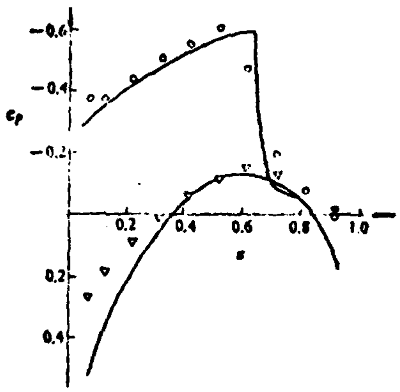

Fig. 5. Constant pressure distribution for a rectangular wing with a 5% double circular-arc airfoil and an aspect ratio of 3.

o upper surface test values[8], ▿ lower surface test values,

——— calculated values for this paper

$M_\infty = 0.9$, $\alpha = 5^\circ$, $y = 0$ supercritical

BIBLIOGRAPHY

[1] Emmons, E. W., The numerical solution of compressible fluid flow problems, NACA TN 932 (1944).

[2] Murman, E. M. and Cole, J. D., Calculation of plane steady transonic flows, *AIAA J*, 9, 1(1971).

[3] Weatherill, W. H., Ehlers, F. E. and Sebastian, J. D., Computation of the transonic perturbation flow fields about two-and three-dimensional osillating wings, NASA CR-2599 (1975).

[4] Newman, P. A. and Kunker, E. B., Computation of transonic flow about finite lifting wings, *AIAA J*, 10, 7(1972).

[5] Knechtel, E. C., Experimental investigation at transonic speeds of pressure distribution over wedge and circular arc airfoil sections, NASA TN D-15 (1959).

[6] Bailey, F. R. and Steger, J. L., Relaxation techniques for three-dimensional transonic flow about wings, AIAA paper 72—189.

[7] Lomax, H., Bailey, F. R. and Ballhaus, W. F., On the numerical simulation of three-dimensional transonic flow with application to the C-141 Wing, NASA TN D-6933 (1973).

[8] Lassing, H., Troutman, J. and Menees, G., Experimental deterimination of the pressure distribution on a rectangular wing osillation in first bending made for Mach numbers from 0.24 to 1.30, NASA TND-344 (1960).